Optics Letters

Reconfigurable microwave photonic mixer with minimized path separation and large suppression of mixing spurs

ZHENZHOU TANG AND SHILONG PAN*

Key Laboratory of Radar Imaging and Microwave Photonics, Ministry of Education, Nanjing University of Aeronautics and Astronautics, Nanjing 210016, China
**Corresponding author: pans@ieee.org*

Received 10 October 2016; revised 30 November 2016; accepted 1 December 2016; posted 1 December 2016 (Doc. ID 278378); published 20 December 2016

A compact reconfigurable photonic microwave mixer is proposed and demonstrated based on a dual-polarization Mach–Zehnder modulator and an optical 90-deg hybrid. By simply changing the photodetection schemes, single-ended, double-balanced, I/Q, and image-reject mixing can be implemented. Thanks to the sidebands selection by an optical filter, unwanted mixing spurs are highly suppressed. In addition, the system is insensitive to environmental vibration because the optical path separation is minimized. An experiment is carried out. Reconfigurable mixing functionalities with very small phase dithering are verified. The mixing spurs are suppressed by more than 30 dB, and the image-reject ratio for image-reject mixing is about 40 dB. © 2016 Optical Society of America

OCIS codes: (060.2330) Fiber optics communications; (070.1170) Analog optical signal processing; (060.5625) Radio frequency photonics.

https://doi.org/10.1364/OL.42.000033

Owing to the advantages of large bandwidth, high isolation, and immunity to electromagnetic interference, the microwave photonic mixer has attracted significant interest in recent years [1–4]. Although various photonic-based methods have been proposed to achieve the microwave mixing [5–9], there are still two key challenges that are difficult to deal with: (1) most of the reported microwave photonic mixers can only achieve the simplest single-ended frequency mixing, other high performance mixers, such as the double-balanced, I/Q, and image-reject mixer, have rarely been implemented in the optical domain; and (2) at the output of the mixer, a lot of unwanted mixing spurs would be generated. The existence of mixing spurs will restrict the operational bandwidth of the microwave photonic mixer. Previously, a few approaches have been reported to solve the two problems [10–14]. To achieve I/Q and image-reject mixing, a pair of quadrature LO signals generated by an electrical 90-deg hybrid are applied to conventional single-ended mixers [10]. However, since the wideband electrical hybrid with precise 90-deg phase shift is hard to obtain, a small operational bandwidth or a low image reject ratio (typically lower than 30 dB) will result. Parallel electro-optical modulation together with an optical 90-deg hybrid can also be applied to achieve the I/Q mixing [11]. When the optical RF signal and optical LO signal produced by the parallel electro-optical modulation are respectively applied to the two input ports of the optical hybrid, an equivalent quadrature phase shift will be introduced to the LO, from which a pair of quadrature IF (intermediate frequency) outputs are obtained after photodetection.

On the other hand, advanced modulation formats are employed to suppress the mixing spurs in the optical domain. For instance, if the double-sideband modulation in [11] is replaced by carrier-suppressed double-sideband (CS-DSB) modulation, the carrier-related LO and RF leakages would be effectively removed, which significantly increases the LO/RF-to-IF isolation [12,13]. Furthermore, with one of the sidebands removed based on carrier-suppressed single-sideband (CS-SSB) modulation, photonic microwave mixing with significantly fewer mixing spurs would be realized [14].

Recently, we proposed a reconfigurable microwave photonic mixer based on CS-SSB modulation and an optical 90-deg hybrid [15]. However, since parallel modulations, parallel filterings, and parallel amplifications are required to obtain the independent RF and LO sidebands, not only is the system complex and costly, but also its performance is vulnerable to differences (in terms of insertion loss, path length, and transmission response) between the two branches. In addition, because the parallel structure is realized by discrete components with relatively long path lengths, fast phase dithering due to the environmental vibration would be a serious problem for practical applications [11].

In this Letter, we propose a compact reconfigurable microwave photonic mixer based on a dual-polarization Mach–Zehnder modulator (DPol-MZM) and an optical 90-deg hybrid. Compared to [15], the parallel signal modulations are implemented in an integrated modulator, which are polarization multiplexed at the output. Therefore, both the RF and LO sidebands can be filtered and amplified by the same optical bandpass filter (OBPF) and erbium-doped fiber amplifier

(EDFA), guaranteeing the link consistency for both signals. Although the RF and LO sidebands have to be separated when introduced to the optical hybrid, the separation lengths can be very small and are easily packaged to isolate them from environmental vibration. A proof-of-concept experiment is carried out. Single-ended, double-balanced, I/Q, and image-reject mixing are successfully implemented. Since only the useful sidebands are selected by the optical filter, the unwanted mixing spurs are largely suppressed.

Figure 1 shows the schematic diagram of the proposed reconfigurable mixer. A continuous-wave light generated by a laser diode (LD) is sent to a DPol-MZM via a first polarization controller (PC1). The DPol-MZM integrates an optical splitter, two sub-MZMs (MZM1 and MZM2), a polarization rotation element and a polarization beam combiner (PBC). In the DPol-MZM, the optical carrier is equally split into two orthogonal branches (X and Y polarizations), and sent to MZM1 and MZM2, respectively. An RF signal with an angular frequency of ω_F is sent to MZM1 and an LO signal with an angular frequency of ω_L is applied to MZM2. The output signals from MZM1 and MZM2 are combined by the PBC. When setting the bias voltages applied to MZM1 and MZM2 to achieve the CS-DSB modulation, the output polarization-multiplexed signal of the DPol-MZM can be expressed as

$$\begin{bmatrix} E_{x1} \\ E_{y1} \end{bmatrix} \propto \begin{bmatrix} jJ_1(\beta_F)\exp(j(\omega_C-\omega_F)t)+jJ_1(\beta_F)\exp(j(\omega_C+\omega_F)t) \\ jJ_1(\beta_L)\exp(j(\omega_C-\omega_L)t)+jJ_1(\beta_L)\exp(j(\omega_C+\omega_L)t) \end{bmatrix}, \tag{1}$$

where ω_C is the angular frequency of the optical carrier, β_F and β_L are the modulation indices. Due to small signal modulation, the higher-order (≥ 2) sidebands are ignored. By using an OBPF, +1st-order RF and LO sidebands are both selected:

$$\begin{bmatrix} E_{x2} \\ E_{y2} \end{bmatrix} \propto \begin{bmatrix} jJ_1(\beta_F)\exp(j(\omega_C+\omega_F)t) \\ jJ_1(\beta_L)\exp(j(\omega_C+\omega_L)t) \end{bmatrix}. \tag{2}$$

The output signal from the OBPF is amplified by an EDFA and sent to a second PC (PC2) and a polarization beam splitter (PBS). By adjusting PC2, the modulated signal in the upper branch (E_{x2}) is output from one output port (X) of the PBS and at the same time the optical signal in the lower branch (E_{y2}) is transmitted to the other output port (Y) of the PBS. Then, the X-port of the PBS is connected to the signal port of an optical 90-deg hybrid, and the Y-port is connected to the LO port of the optical hybrid. The signals from the four output ports of the optical hybrid can be written as

$$\begin{aligned} I_1 &\propto jJ_1(\beta_F)\exp[j(\omega_C+\omega_F)t]+jJ_1(\beta_L)\exp[j(\omega_C+\omega_L)t], \\ I_2 &\propto jJ_1(\beta_F)\exp[j(\omega_C+\omega_F)t]-jJ_1(\beta_L)\exp[j(\omega_C+\omega_L)t], \\ Q_1 &\propto jJ_1(\beta_F)\exp[j(\omega_C+\omega_F)t]-J_1(\beta_L)\exp[j(\omega_C+\omega_L)t], \\ Q_2 &\propto jJ_1(\beta_F)\exp[j(\omega_C+\omega_F)t]+J_1(\beta_L)\exp[j(\omega_C+\omega_L)t], \end{aligned} \tag{3}$$

where $I_{1,2}$ denote the in-phase outputs and $Q_{1,2}$ represent the quadrature outputs. If each of the output signals is sent to a photodetector (PD), the time-varying terms of the detected photocurrents are given by

$$\begin{aligned} i_{I_1} &\propto +J_1(\beta_F)J_1(\beta_L)\cos[(\omega_F-\omega_L)t], \\ i_{I_2} &\propto -J_1(\beta_F)J_1(\beta_L)\cos[(\omega_F-\omega_L)t], \\ i_{Q_1} &\propto -J_1(\beta_F)J_1(\beta_L)\sin[(\omega_F-\omega_L)t], \\ i_{Q_2} &\propto +J_1(\beta_F)J_1(\beta_L)\sin[(\omega_F-\omega_L)t]. \end{aligned} \tag{4}$$

As can be seen from Eq. (4), each of the outputs can be viewed as a single-ended frequency mixer. Because $i_{I1}(i_{I2})$ and $i_{Q1}(i_{Q2})$ have a phase difference of $\pm\pi/2$, an I/Q frequency mixer can also be naturally realized. Based on the I/Q mixer, when these two outputs of the I/Q mixer are combined by a low-frequency IF electrical quadrature hybrid, an image-reject mixer could be achieved. In addition, since i_{I1} and i_{I2} (or i_{Q1} and i_{Q2}) are 180° out of phase, a double-balanced frequency mixer can be achieved if a balanced PD is connected to the in-phase (or quadrature) output ports. Since the optical filter only selects the two 1st-order RF and LO sidebands, only the desired frequency-converted signals would be generated, which means that mixing spurs could be largely suppressed.

A proof-of-concept experiment based on Fig. 1 was carried out. An optical carrier with a wavelength of 1550.5 nm and a power of 16 dBm is generated by a LD (Teraxion

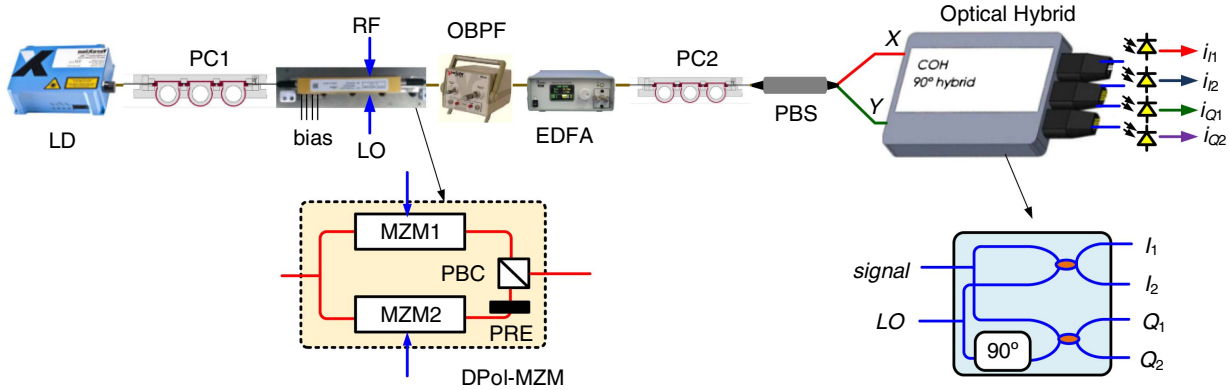

Fig. 1. Schematic diagram of the proposed reconfigurable mixer. LD, laser diode; PC, polarization controller; DPol-MZM, dual-polarization Mach–Zehnder modulator; OBPF, optical bandpass filter; EDFA, erbium-doped fiber amplifier; PBS, polarization beam splitter; PBC, polarization beam combiner; PRE, polarization rotation element.

PS-NLL-1550.52-80-04) and sent to a DPol-MZM (Fujitsu FTM7980) via a PC. A RF signal generated by a vector signal generator (Agilent E8267D) and an LO signal produced by an analog signal generator (Agilent E8257D) are sent to MZM1 and MZM2, respectively. An OBPF (Yenasta XTM-50) is used to select both the +1st-order RF and LO sidebands. The output signal from the OBPF is amplified by an EDFA (Amonics Inc.) and polarization demultiplexed by PC2 and a PBS. The two outputs of the PBS are connected to the signal port and LO port of an optical 90-deg hybrid (Kylia COH28), respectively. The optical spectrum is measured by an optical spectrum analyzer (YOKOGAWA AQ6370C) and the electrical spectrum is observed by a 43-GHz electrical signal analyzer (Agilent N9030A). In addition, a 32-GHz four-channel digital oscilloscope (Agilent DSO-X 92504A) is used to observe the electrical waveforms.

In the first step of the experiment, the frequencies of the RF and LO signals are set to 21 and 20 GHz, respectively. The optical spectrum of the modulated signal is shown as the dashed line in Fig. 2. When properly setting the bias voltages applied to MZM1 and MZM2, a CS-DSB modulated signal would be obtained (dashed–dotted line). As can be seen, the carrier is suppressed by 40 dB. By the OBPF with a frequency response shown as the short-dashed line in Fig. 2, only the positive LO and RF sidebands are selected (solid line). The output signal from the OBPF is amplified by the EDFA and then polarization demultiplexed into two orthogonal parts. Figure 3 shows the optical spectra measured at the two output ports of the PBS. The RF and LO sidebands can be easily distinguished, indicating that effective polarization multiplexing and demultiplexing are achieved.

When I_1 and I_2 of the optical hybrid are sent to two PDs (u2t 2120RA) with bandwidths of 45 GHz and responsivities of 0.65 A/W, the waveforms of i_{I1} (solid line) and i_{I2} (dashed line) are shown in Fig. 4(a). As can be seen, the waveforms of i_{I1} and i_{I2} have almost identical amplitude and a phase difference of 180 deg, which means a double-balanced mixer is realized. Similarly, when I_1 and Q_1 are sent to the PDs, the obtained waveforms are presented in Fig. 4(b). Compared to i_{I1} (solid line), the waveform of i_{Q1} (dashed line) has the same amplitude but with a quadrature phase difference, indicating that an I/Q mixer can be obtained. When i_{I1} and i_{Q1} are combined by an electrical 90-deg quadrature hybrid (Krytar 3017360 K), the waveform and electrical spectrum of the combined signal are shown as the solid lines in Figs. 5(a) and 5(b), respectively. From the electrical spectrum, a −25 dBm IF signal

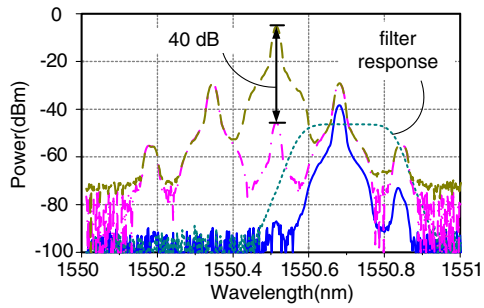

Fig. 2. Optical spectra of the modulated signal without carrier suppression (dashed line), with carrier suppression (dashed–dotted line), and after optical filtering (solid line) by the OBPF. Short-dashed line: response of the OBPF.

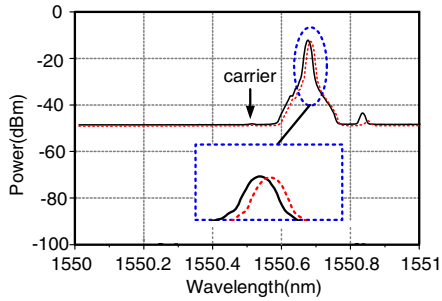

Fig. 3. Optical spectra of +1st-order RF sideband (dashed line) and LO sideband (solid line). Inset: zoom-in view of the peaks.

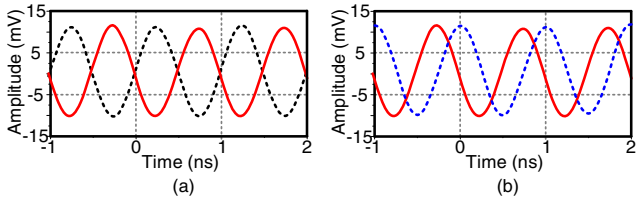

Fig. 4. (a) Electrical waveforms of i_{I1} (solid line) and i_{I2} (dashed-line) and (b) electrical waveforms of i_{I1} (solid line) and i_{Q1} (dashed line).

at the frequency of 1 GHz is obtained. To demonstrate the image rejection, the frequency of the RF signal is changed to be the image frequency (i.e., 19 GHz). The corresponding waveform and spectrum are shown as the dashed lines in Figs. 5(a) and 5(b). The amplitude of the downconverted signal, as can be seen from Fig. 5(a), is nearly zero, and the power is about −65 dBm, showing that an image-reject ratio of 40 dB is achieved. Compared to [15], the polarization cross talk between the X- and Y-polarized paths of the PBS should be taken into consideration since it would influence the image-reject ratio of the image-reject mixer. To investigate this influence, the X- (and Y-) polarized output of the PBS is sent to a PD directly. Figures 6(a) and 6(b) show the detected electrical spectra. As can be seen, since the optical carrier is removed by the optical filter, the RF (or LO) signal would not be generated. However, due to the polarization cross talk of the PBS, the RF sideband (or LO sideband) would leak to the other branch, which would generate an unwanted IF component at the PD. The powers of the obtained IF components are around −65 dBm. Since the IF components generated by the polarization cross talk come from the optical signals before the optical hybrid, they would have the same phase, which cannot be suppressed using the phase cancellation method. The polarization cross talk can be reduced by employing a

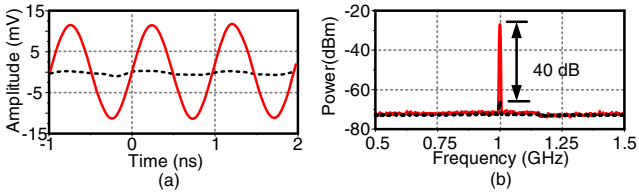

Fig. 5. (a) Waveforms of the IF signals downconverted from the RF signal (solid line) and the image (dashed line) and (b) the corresponding electrical spectra.

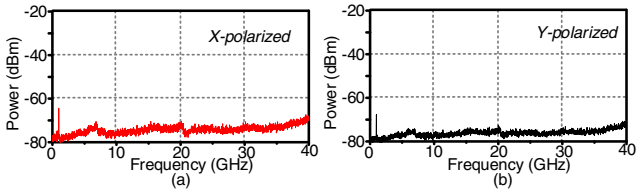

Fig. 6. Measured electrical spectra when (a) X-polarized and (b) Y-polarized branches of the PBS are sent to a PD directly.

PBS with high polarization isolation ratio. Another main factor that can affect the image-reject ratio is the amplitude and phase imbalance of the quadrature outputs of the optical hybrid, which can be reduced by inserting an optical variable attenuator and an optical tunable delay line [16].

Thanks to the RF and LO sidebands selection by the OBPF, the mixing spurs are largely suppressed. Figure 7(a) shows the electrical spectrum of the downconverted 1-GHz IF signal. Only the desired frequency component can be observed, and the power of the mixing spurs are 30 dB lower than that of the 1-GHz signal. Figure 7(b) depicts the electrical spectra of the IF signals when the LO frequency is fixed at 20 GHz and the RF signal is tuned from 21 to 39 GHz. As can be seen, wideband frequency mixing with large suppression of mixing spurs is achieved. The powers of the generated IF signals are not identical, since the frequency responses of the modulator, the PDs, and the microwave components are not flat within the operational bandwidths.

Table 1 summarizes the measured key parameters of the proposed mixer. The lower limit of the LO/RF bandwidth is restricted by the roll-off factor of the OBPF used in the experiment, which is about 500 dB/nm. According to [15], the lower limit is 10 GHz. On the other hand, the upper limit of the RF/LO bandwidth is dependent on the modulation bandwidth of the DPol-MZM, which is about 40 GHz. For a given conversion loss of 30 ± 3 dB, the measured IF bandwidth is DC-12 GHz. It should be noted that the conversion loss can be reduced by increasing the gain of the EDFA [8]. The mixing spurs are suppressed by more than 30 dB. When performing the image-reject mixing, the image-reject suppression ratio is around 40 dB.

The influence of the environmental vibration is also evaluated. Since the parallel RF and LO modulations are implemented by an integrated modulator, and the modulated RF and LO sidebands are filtered and amplified by the same OBPF and EDFA, the consistency of link performance for both RF and LO signals is easily guaranteed. Although the RF and LO sidebands have to be separated by the PBS before connecting to the optical hybrid, the lengths of the pigtails are short and nearly identical. In the experiment, the waveforms in Figs. 4 and 5 are monitored for 60 min, and only very small phase dithering is

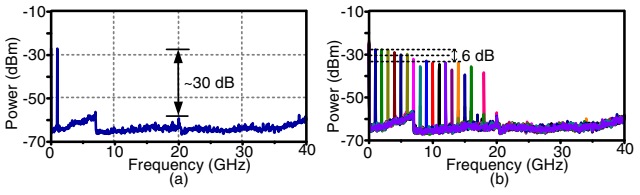

Fig. 7. (a) The spectrum of the 1-GHz IF signal and (b) the spectra of the IF signals when LO is 20 GHz and RF is tuned from 21 to 39 GHz.

Table 1. Parameters of the Reconfigurable Mixer

Parameter	Value
Conversion loss	30 ± 3 dB
RF/LO bandwidth	10–40 GHz
IF bandwidth	DC–12 GHz
Spur suppression	>30 dB
Image rejection ratio	~40 dB

observed. It should be noted that the PBS can be well packaged or integrated into the optical hybrid, so the stability of the mixer can be further improved.

In conclusion, a stable and reconfigurable microwave photonic mixer with large suppression of mixing spurs and minimized path separation is proposed based on a DPol-MZM and an optical 90-deg hybrid. A proof-of-concept experiment is carried out. Single-ended, balanced, I/Q, and image-reject mixing are realized based on the proposed mixer. The measured image-reject ratio is about 40 dB and the mixing spurs are suppressed by more than 30 dB. The proposed mixer features simple configuration, flexible functionalities, and stable operation, which can find applications in broadband and multifunctional microwave photonic systems.

Funding. National Natural Science Foundation of China (NSFC) (61422108, 61527820); Fundamental Research Funds for the Central Universities; Priority Academic Program Development of Jiangsu Higher Education Institutions; Nanjing University of Aeronautics and Astronautics (NUAA) (BCXJ16-04).

REFERENCES

1. K. Gopalakrishnan, W. K. Burns, and C. H. Bulmer, IEEE Trans. Microwave Theory Tech. **41**, 2383 (1993).
2. B. Benazet, M. Sotom, M. Maignan, and J. Perdigues, Proc. SPIE **6194**, 619403 (2006).
3. M. E. Manka, *International Topical Meeting on Microwave Photonics (MWP) Jointly Held with the 2008 Asia-Pacific Microwave Photonics Conference (APMP)* (2008), pp. 275–278.
4. S. L. Pan, D. Zhu, S. F. Liu, K. Xu, Y. T. Dai, T. L. Wang, J. G. Liu, N. H. Zhu, Y. Xue, and N. J. Liu, IEEE Microwave Mag. **16**(8), 61 (2015).
5. P. W. Juodawlkis, J. J. Hargreaves, R. D. Younger, G. W. Titi, and J. C. Twichell, J. Lightwave Technol. **21**, 3116 (2003).
6. C. Bohemond, T. Rampone, and A. Sharaiha, J. Lightwave Technol. **29**, 2402 (2011).
7. S. N. Fu, W. D. Zhong, P. Shum, Y. J. Wen, and M. Tang, IEEE Photon. Technol. Lett. **21**, 563 (2009).
8. E. H. W. Chan and R. A. Minasian, J. Lightwave Technol. **30**, 3580 (2012).
9. V. R. Pagán, B. M. Haas, and T. Murphy, Opt. Express **19**, 883 (2011).
10. C. Lu, W. Y. Chen, and J. F. Shiang, IEEE Trans. Microwave Theory Tech. **45**, 1478 (1997).
11. S. R. O'Connor, M. C. Gross, M. L. Dennis, and T. R. Clark, *IEEE Topical Meeting on Microwave Photonics (MWP)* (2009), p. 1.
12. Z. Z. Tang, F. Z. Zhang, D. Zhu, X. H. Zou, and S. L. Pan, *IEEE Topical Meeting on Microwave Photonics (MWP)* (2013), p. 150.
13. Z. Z. Tang, F. Z. Zhang, and S. L. Pan, Opt. Express **22**, 305 (2014).
14. Z. Z. Tang and S. L. Pan, IEEE Microwave Wireless Compon. Lett. **26**, 67 (2016).
15. Z. Z. Tang and S. L. Pan, IEEE Trans. Microwave Theory Tech. **64**, 3017 (2016).
16. J. Zhang, E. H. W. Chan, X. Wang, X. Feng, and B. Guan, IEEE Photon. J. **8**, 3900411 (2016).

1557-9638/18/$15.00 © 2018 IEEE